Geometry Retrieval From CT and MRI of the Human Upper Airways

Maria Rolstad Jordal

December 18, 2015

Preface

This project work is a part of a larger research project "Modeling of Obstructive Sleep Apnea by Fluid-Structure Interaction in the Upper Airways" which is a collaboration project between NTNU, SINTEF and St Olav University Hospital. It is funded by NTNU and the Research Council of Norway [1, 2]. The aim of this project is "to demonstrate the potential of a new patient-specific clinical tool based on mathematical models in predicting the response to Obstructive Sleep Apnea Syndrome (OSAS) treatment" [2].

At St Olav University Hospital in Trondheim, Norway, intranasal surgery is being performed on patients with OSAS, but only one third of the patients experience improvement in OSAS after surgery. It is not known why there is such a low success rate after surgery and why some patients improve and others do not [3]. By studying the geometry and flow patterns of the upper airways before and after surgery, the impact of intranasal surgery on the airflow in the upper airway might become clearer.

The main project is subdivided into four workpackages (WP); Clinical Research (WP1), Soft Tissue Modelling (WP2), Mathematical Modelling of Fluid-Structure Interaction (WP3) and Computation Fluid Dynamics (CFD) Modelling for Prediction of Success of OSAS Surgery (WP4). This project work is a part of WP4.

I would like to thank my supervisor prof. Bernhard Müller (NTNU) and my two co-supervisors Sigrid Kaarstad Dahl (SINTEF MK) and Sverre Gullikstad Johnsen (SINTEF MK) for guidance and motivation throughout the entire process. I would also like to thank dr. Mads Henrik Strand Moxness (Aleris) for helping out with the segmentation and explaining the physiology of the upper airways. In addition, I would like to thank dr. Kjell Arne Kvistad (St.Olav) for explaining the CT and MRI procedure and helping me out with the segmentation.

Abstract

Obstructive Sleep Apnea Syndrome (OSAS) is a common and serious disorder where obstructions in the upper airways prevents the air from flowing freely during sleep. At St. Olav Unversity Hospital, intranasal surgery is being performed on patients with clinically significant nasal obstructions for alleviation of OSAS, but only one third of the patients improve in OSAS. In an ongoing research project "Modeling of Obstructive Sleep Apnea by Fluid-Structure Interaction in the Upper Airways" the aim is to make a patient-specific mathematical tool to predict the outcome of these surgeries. To do so, the flow pattern in the upper airways will be studied, and this report suggests a protocol for geometry retrieval from MRI (Magnetic Resonance Imaging) and CT (Computed Tomography) obtained from the patients before and after surgery.

The model is based entirely on the datasets from CT as they were of better quality than the MRI datasets and also easier to segment. The segmentation was done in ITK-SNAP 3.2.0 with a combination of automatic and manual procedure. For the automatic segmentation, thresholding was used with no lower limit and an upper limit of -300 HU. Manual segmentation was needed to get accurate results - especially in the nasal cavities. A clinician must also be involved in the segmentation procedure to ensure that the segmented volume corresponds well with the anatomy seen in the CT scans. The model was extracted as a surface mesh, and converted into a solid body in FreeCAD. The solid body was imported to ANSYS DesignModeler to be partitioned. The partitioned model was further imported to ANSYS Meshing for grid generation.

In addition to developing the workflow for geometry retrieval and grid generation mentioned, a protocol for CT image acquisition was also developed. To be able to compare the airflow in the upper airways before and after surgery, the data from the CT scans must be comparable. At the moment they are not, but from now on the images will be taken with the patient in the same position, and with both an open and a closed mouth.

The protocols for image acquisition, geometry retrieval and grid generation are the outcomes of this project. To validate the model made (including geometry and grid), flow simulations are needed. As of now it is not possible to estimate the accuracy of the model.

Contents

Preface i

Abstract iii

1. Introduction 3
1.1 Computational Fluid Dynamics in Medicine . . . 3
1.2 Anatomy of the Human Upper Airways . . . 4
1.2.1 Definition of the Anatomical Planes and Directions . . . 5
1.2.2 The Nose, Nasal Cavity and Sinuses . . . 5
1.2.3 Pharynx . . . 6
1.2.4 Larynx . . . 7
1.3 Obstructive Sleep Apnea Syndrome . . . 7
1.3.1 Characteristics . . . 8
1.3.2 Biologic Basis . . . 8
1.3.3 Risk factors for OSAS . . . 9
1.3.4 Complications and Associations . . . 9
1.3.5 Available Treatments . . . 10
1.4 Medical Imaging . . . 10
1.4.1 MRI . . . 11
1.4.2 CT . . . 12
1.5 Geometry Retrieval . . . 13
1.6 Grid Generation . . . 13
1.6.1 Grid Characteristics . . . 14
1.6.2 Evaluation of grid quality . . . 14

2. Method 15
2.1 Geometry Retrieval . . . 15
2.1.1 Data Acquisition . . . 15
2.1.2 Choice of medical image procedure . . . 15
2.1.3 Segmentation . . . 16
2.1.4 Conversion from surface mesh to solid body . . . 22
2.2 Grid Generation . . . 22
2.2.1 Choice of grid type . . . 22
2.2.2 Generating the grid . . . 22

3. Results 25
3.1 Geometry . . . 25
3.2 Grid . . . 27
3.3 Protocol . . . 31

4. Discussion 35

5. Conclusions 39

6. Further Work 41

1. Introduction

The objective of this project work is to develop a method for creating "patient-specific three-dimensional computational models of the human upper airways based on Magnetic Resonance Imaging (MRI) and Computed Tomography (CT) scans" [2]. When a reliable method is developed, models of the upper airways of several patients can be made both pre- and post-operatively to further investigate the impact of nasal surgery on Obstructive Sleep Apnea Syndrome (OSAS).
To be able to do the Computational Fluid Dynamics (CFD) modelling in Work Package (WP) 4 "Modeling for Prediction of Success of OSAS Surgery" of the research project "Modeling of Obstructive Sleep Apnea by Fluid-Structure Interaction in the Upper Airways" [1,2], the first step is to obtain a geometry of the human upper airway. MRI and CT of the patients were obtained in WP1 "Clinical Research" of [1, 2], and this project work aims to extract the airway geometry from those medical images. In addition to obtaining a geometry, this project work will also include grid generation of the model for further CFD modelling.

Some theoretical background is necessary to understand the purpose of the study and be able to create a model. Chapter 1.3 explains the anatomy of the upper airways needed to model it correctly and understand OSAS. The physiology of OSAS is further being explained in chapter 1.4. Risk factors, treatment and complications associated with OSAS will also be explained in the same chapter. Chapter 1.5 is about the physics behind the medical images and the data they contain. Chapter 1.6 and 1.7 give a brief introduction to geometry retrieval and grid generation.

1.1 Computational Fluid Dynamics in Medicine

CFD has become a bigger part of medical research as a result of improvement in technology aiding medical image acquisition and segmentation, grid generation, and flow calculations [4]. The technology improvement also lowered the computational cost of the simulation significantly which makes CFD a much more desirable tool now than before.

Using CFD to predict the outcome of a surgery is still a relatively new research area and is not in clinical use. However, results so far predict CFD to be a helpful tool for predicting the outcome of surgery in the upper airways [5, 6].

1.2 Anatomy of the Human Upper Airways

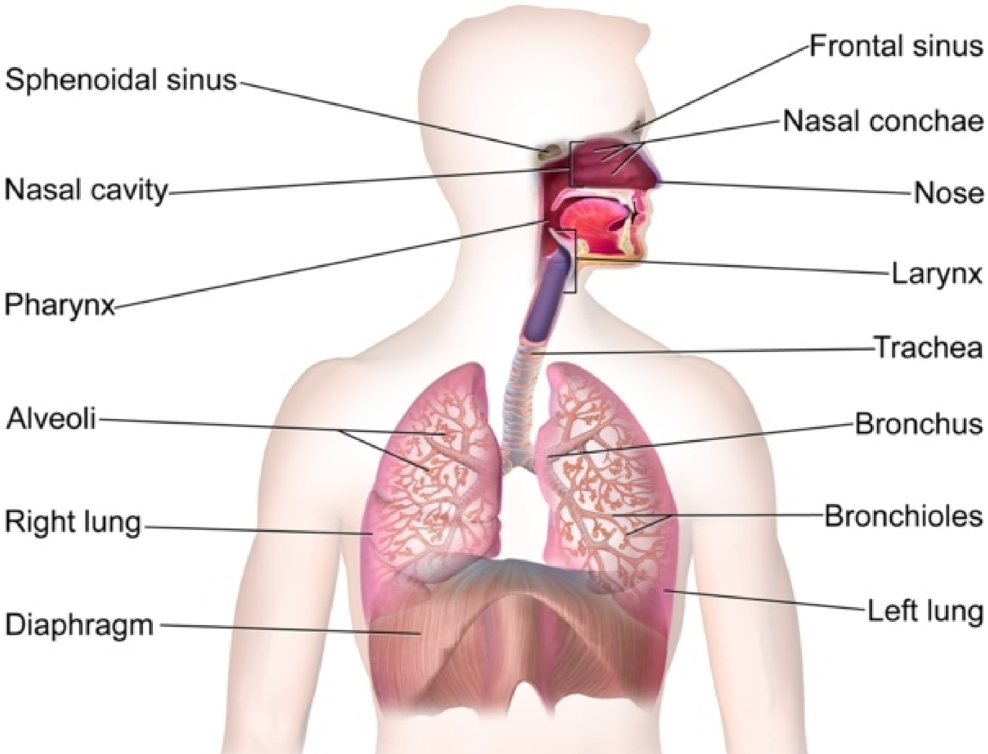

Figure 1: Schematic of the respiratory system [7]

.

The main function of the human respiratory system is to exchange the oxygen inhaled from air with carbon dioxide in the blood. The respiratory system can be divided into the upper- and lower respiratory tract where the lower airway includes organs within the chest cavity, while the upper airway includes the organs outside of it. The dividing of the respiratory system is also based on its functions. Air is first inhaled through the nose and mouth and gets warmed, humidified and filtered in the upper respiratory system. As the air enters the lower respiratory system, the gas exchange takes place in the alveoli (Fig. 1). After the gas exchange, the air, that is now containing carbon dioxide, will be exhaled through the upper respiratory system. This exchange happens on every inhalation and exhalation. Other main functions of the respiratory system are sound production, smell and control of body pH-levels [8].

For the case of OSAS, only the upper respiratory system is of interest. A more detailed description of the anatomy will be presented in the following subsections.

The human upper airways begin at the nose and end at the beginning of trachea. The upper airway consists of the main components; the nose and nasal cavity, the mouth and oral cavity, the pharynx and the larynx (Fig. 1). Study of the airflow for OSAS patients is best done when the mouth is closed, hence the physiology of the mouth will not be explained further in this section.

1.2.1 Definition of the Anatomical Planes and Directions

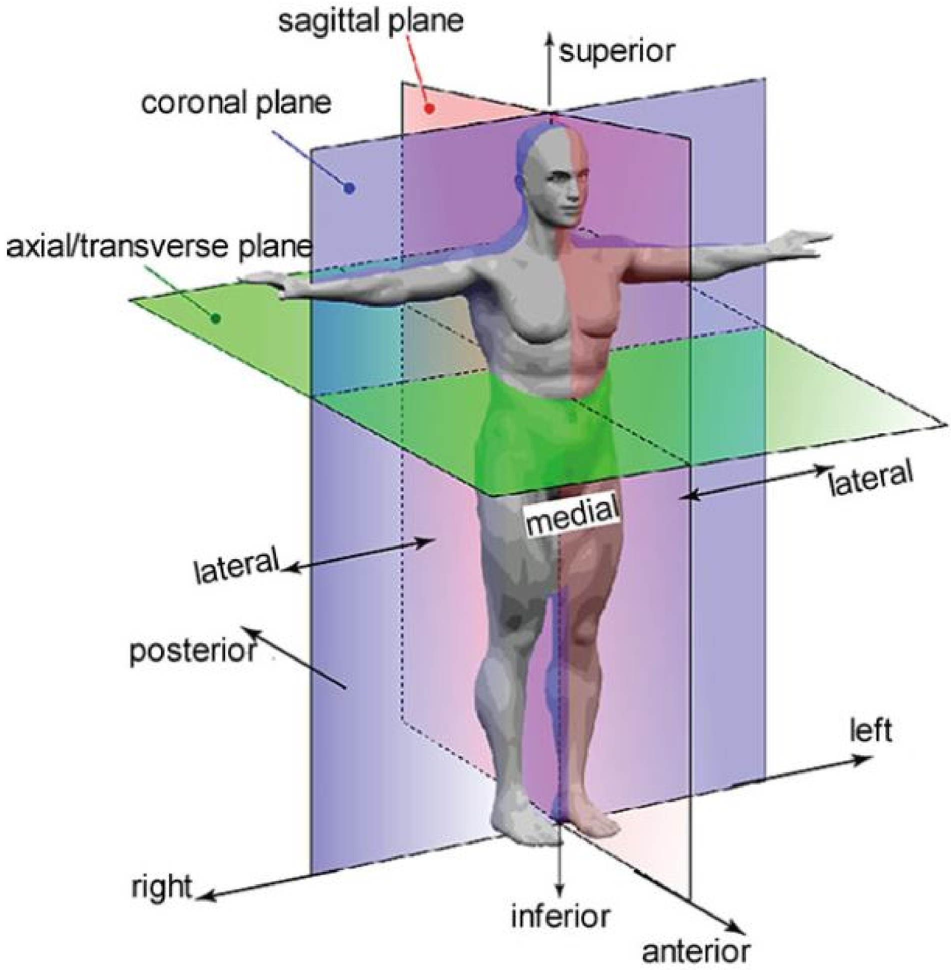

Figure 2: The anatomical planes and position definition [8].

Fig. 2 shows the definitions of the anatomical planes and directions. These definitions will be used throughout the report.

1.2.2 The Nose, Nasal Cavity and Sinuses

The first part of the upper respiratory tract is the nose which is both air inlet and outlet for inhalation and exhalation, respectively.

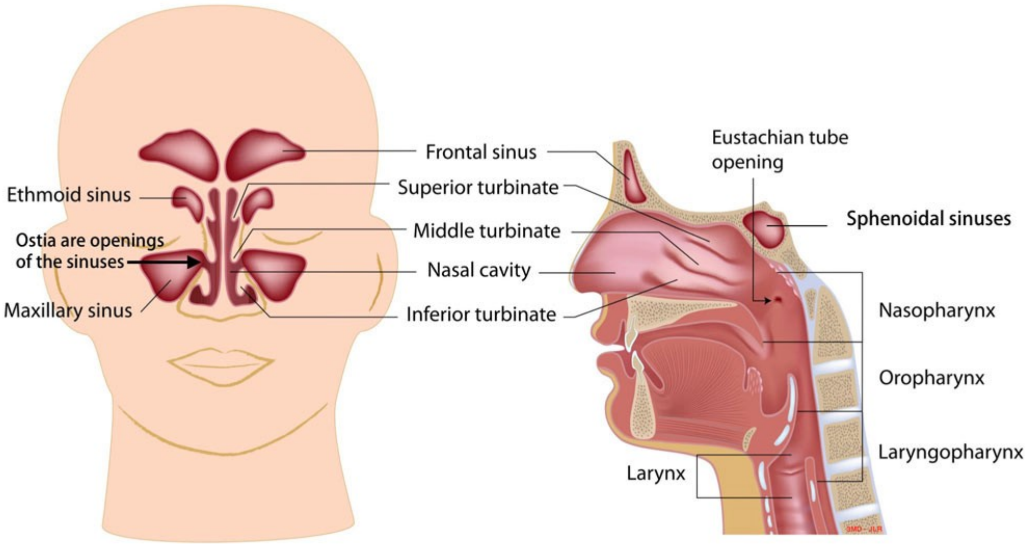

Figure 3: Schematic view of the upper respiratory tract, coronal (left) and sagittal (right) plane [9].

Air enters the nares (also called nostrils) and flows into the two nasal cavities. Breathing can be affected of the nasal cycle, which is a phenomena observed in about 80% of the normal individuals. During each nasal cycle, one of the nasal passages is dominant causing the airflow through the nasal cavities to be asymmetrical. Each cycle last from 30 minutes to 6 hours [8]. The nasal cavities are separated by nasal septum cartilage. The nasal septum is in most cases straight, but a deviated septum is common and often caused by some external trauma [10]. In each of the nasal cavities there are three (rarely four) turbinates/conchaes; the inferior, middle and superior turbinate. These are scroll-like projections from the lateral nose wall that regulate, humidify, filter, pressurize, elevate and streamline the air [11]. The nasal cavity is connected to the paranasal sinuses by small channels. The paranasal sinuses are air-filled spaces and consist of four pairs of sinuses; the frontal, sphenoid, ethmoid and maxillary sinuses (Fig. 3). The functions of the paranasal sinuses is speculative, but they do add resonance to the voice and decrease the weight of the skull [10].

1.2.3 Pharynx

The pharynx is a tube like structure that extends from the cranial base to the level of the sixth cervical vertebra and consists partly of collapsible walls [10]. As both food and air pass through the pharynx, it is part of both the digestive and the respiratory system.

The pharynx can be divided into three subdivisons; the nasopharynx, oropharynx and laryngopharynx (sometimes referred to as the hypopharynx) as shown in Fig. 3. The nasopharynx is located above the soft palate and behind the posterior nares. The soft palate faces upward during swallowing, preventing food and air to enter the nasopharynx. Inferior of the soft palate and posterior to the mouth is the oropharynx. This goes all the way down to the hyoid bone which also marks the upper boundary of the epiglottis. Both food and air pass through the oropharynx and are later separated by the epiglottis in the laryngopharynx. The laryngopharynx is located between the hyoid bone and at the junction where the airway splits into the trachea and oesophagus and becomes continuous with the oesophagus [10].

1.2.4 Larynx

The larynx (also known as the voice box) is an air passage and serves as a sphincter that transmits air from the oropharynx to the tranchea (see Fig. 3) and creates sound for speech [10].

1.3 Obstructive Sleep Apnea Syndrome

Even though OSAS is a common and serious disease, it is quite new as a research area as the syndrome itself was not recognized until advances in technology made it possible to measure the symptoms.

The first description of a syndrome similar to OSAS in literature is found in Charles Dickens "The Pickwick Papers" (1836) where an obese (overweight) boy is struggling with daytime sleepiness and heavy snoring. This character gave name to the "Pickwickian Syndrome" which was a term widely used after Burwell et. al. 1956 [12] described the syndrome in their case study of an obese man struggling with daytime sleepiness. The Picwickian Syndrome became known as Obesity Hypoventilation Syndrome (OHS) afterwards. Characteristics of OHS/The Pickwickian Syndrome is similar to those of OSAS as approximately 90% of those with OHS also have OSAS [13], but the subject is always obese when being affected by OHS. In 1966, Gastaut et al. [14] published a paper observing two "Picwickian" patients and documented that the apneas are cyclic. Further they suggested somnolence as either being caused by a primary disturbance of the brain stem centres that regulates wakefulness and sleep, where the disturbance is somehow linked to obesity, or as a result of the low quality of sleep during night. In the same paper, Gastaut et al. [14] also suggested the respiratory disturbances were caused by a mechanism obstructing the upper outlet of the airflow and in particularly a backward movement of the tongue, which today is known to be a common obstruction for patients with OSAS [15, 16].

During the 1960's and 1970's, tracheostomy was the only available treatment, but not a desired one. However, in 1981 Sullivan et al. [17] introduced and documented the effect of Continuous Positive Airway Pressure (CPAP) on OSAS patients and revolutionized the treatment of OSAS. After this, OSAS has become a research area of interest, and numerous papers on OSAS and its treatment options have been published.

1.3.1 Characteristics

Obstructive sleep apnea syndrome (OSAS) is characterized by an obstruction in the upper airway preventing the air from flowing freely, causing apneas (pauses in breath) during sleep and a lack in the quality of sleep. The most prevalent symptoms are daytime sleepiness, snoring and unrefreshing sleep [15].

The severity of OSAS is characterized by the number of apnea/hypopnea(shallow breathing) events per hour during sleep, which defines the apnea-hypopnea index (AHI). To count as an event, the apnea/hypopnea must exceed 10 seconds. An AHI less than five is considered normal, between 5 and 15 is considered as mild OSAS, between 15 and 30 is moderate OSAS and above 30 is defined as severe OSAS [18]. The Epworth Sleepiness Scale (ESS) is another method used to assess the severity of OSAS. On the ESS, the patient reports the likelihood from 0-3 of falling asleep during eight everyday scenarios [15], hence it is less accurate as it is not measurable.

1.3.2 Biologic Basis

The basis of OSAS is a narrowing and closing of the airway, usually in the oropharynx where the airway is naturally narrow, preventing the air from flowing freely to the lower respiratory tract. As a result of this, the gas exchange in the alveoli does not function properly and the patient experiences hypoxaemia(low concentration of oxygen in the blood) and hypercapnia(high concentration of carbon-dioxide in the blood). The only way to establish airway patency again is arousal from sleep [19].

A narrow airway can be caused by an increased volume in the soft palate or tongue, parapharyngeal fat pads or the lateral walls surrounding the pharynx. During sleep, the muscles are less active and a collapse in the oropharynx can occur as shown in Figure 4. The sleep position of the patient is also of interest. The pharynx has no fixed rigid support, and all the collapsible walls, the soft-palate and tongue move posterior when sleeping on the back because of gravity. Because of this, changing sleeping position can have an effect on the volume of the pharynx [20].

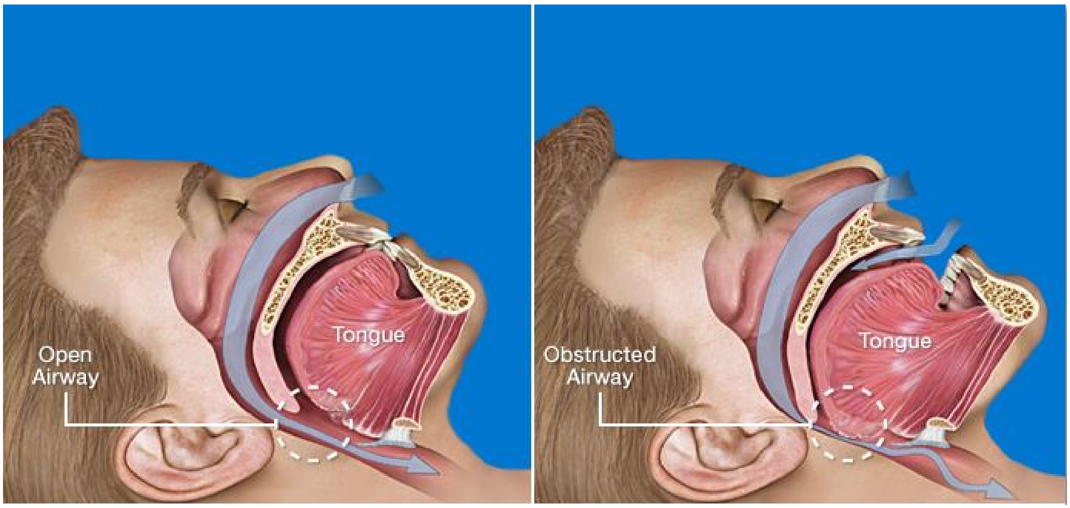

Figure 4: Non-obstructed (left) and obstructed airway (right) [21].

Another cause of obstruction can be observed further up in the nasal cavity where a deviated septum and/or enlargement of the turbinates prevent the air from flowing and causing an airway flow resistance. The low airway pressure also causes the pharyngeal airway to collapse.

1.3.3 Risk factors for OSAS

It is estimated that approximately 2% of middle aged women and 4% of middle aged men suffer from OSAS. OSAS can be caused by different types of obstructions, and there are therefore several different risk factors. One of the most common risk factors are obesity [15]. The following predisposing factors are pointed out by the American Academy of Sleep Medicine [18]; obesity (particularly in the upper body), male gender, craniofacial abnormalities, increased pharyngeal soft tissue, nasal obstruction and familial history. In additon - having a short and wide neck is also a risk factor.

1.3.4 Complications and Associations

The poor quality of sleep caused by OSAS leads to a series of other health issues such as increased risk of cardiovascular diseases, diabetes and depression [15]. Subjects with untreated OSAS also have daily struggles because of the excessive daytime sleepiness. They are in worst case unable to work as they are not able to stay awake and/or function properly during the work day. The unemployment is an economic burden on the society and a burden for the subject itself. OSAS patients are also more likely to have work accidents and get into driving accidents because of their lessened ability to keep focused. Healthcare costs are also higher for OSAS patients, but these costs are however reduced when they are treated with success [22].

1.3.5 Available Treatments

Today there exist several treatments for OSAS. However the response to them differs between the patients based.

One of the first treatments for OSAS was tracheostomy where a tube is inserted into the trachea through the neck. This creates an airway outlet and avoids the problem with obstructions in the upper airway. Tracheostomy is a very effective and successful method, but is only used in special cases or if the patient does not respond to any of the other available treatments. Reasons for avoiding this treatment include inability to swim, unsightly appearance, frequent coughing up of mucous, formation of granulation tissue, aspiration, pneumonia and vocal cord paralysis [23].

Other surgical approaches for OSAS can also be performed to open up the airway depending on what causes the obstructions. Intranasal surgeries such as straightening of the septum or decrease of the turbinates or tissue removal from the soft palate, uvula, tonsils, adenoids or tongue will increase the airway volume. Often, a combination of surgeries is needed for alleviation of OSAS. Surgery to change craniofacial structures can also be performed, but are more complex than the above mentioned surgeries [24].

Continuous Positive Airway Pressure (CPAP) is the standard treatment to OSAS as most patients respond well to this treatment and it does not involve surgery. With CPAP treatment a mask is placed either over the nose, in the nares or over both nose and mouth and a steady stream of positive pressurized air is provided through the mask. The CPAP prevents the pharyngeal airway from collapsing during sleep and therefore reduces the apneas remarkably and daytime sleepiness is reduced/non-apparent. Some patients do however find it impractical to use the mask every night and prefer surgery instead [15].

OSAS can be a result of obesity, and studies have shown that OSAS is more prevalent in the obese and overweight part of the population. Losing weight will in some cases alleviate OSAS as the fat around the pharynx will decrease with the the weight loss and allow the air to flow freely in the pharynx [15].

1.4 Medical Imaging

Medical imaging is a non-invasive technique which can provide a visualization of the interior of the body. There are several types of medical imaging, but only MRI and CT will be considered in this report.

MRI and CT are two kinds of medical imaging that both provide 3D volumetric data from a series of 2D pictures with a specified slice thickness. As seen in Fig. 5, the 2D-slices make up voxels which are 3D-elements defined as the surface area of the pixels extruded between the slices [8].

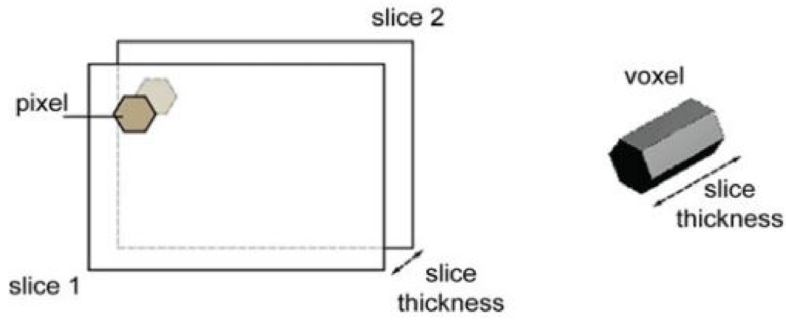

Figure 5: Representation of pixel (2D) and voxel (3D) [8].

1.4.1 MRI

MRI is based upon the fact that the body is largely composed of water and lipid and uses radio waves and magnetic fields to get a distribution map of the hydrogen nucleus/protons in the body [25].

Each hydrogen atom contains a nuclei which has both angular momentum and magnetic moment. The magnitude of these values is fixed, but the directions are random. In an MRI machine, a strong magnetic field (usually 1-3 Tesla) is imposed causing all the protons to align in the same or exact opposite direction with respect to the direction of the magnetic field. A radio frequency pulse is then sent through the body, flipping the spin of the nuclei and when the signal is stopped, the protons will return to their original orientation emitting their own radio signals in the process. It is this radio signal ("echo") that the scanner detects and makes use of. The relaxation time is the time it takes the proton to return to its original state, and both longitudinal (T1) and transverse (T2) relaxation are of interest, as they provide different information for the various tissues [25]. The difference between T1 and T2 can be seen in Fig. 6.

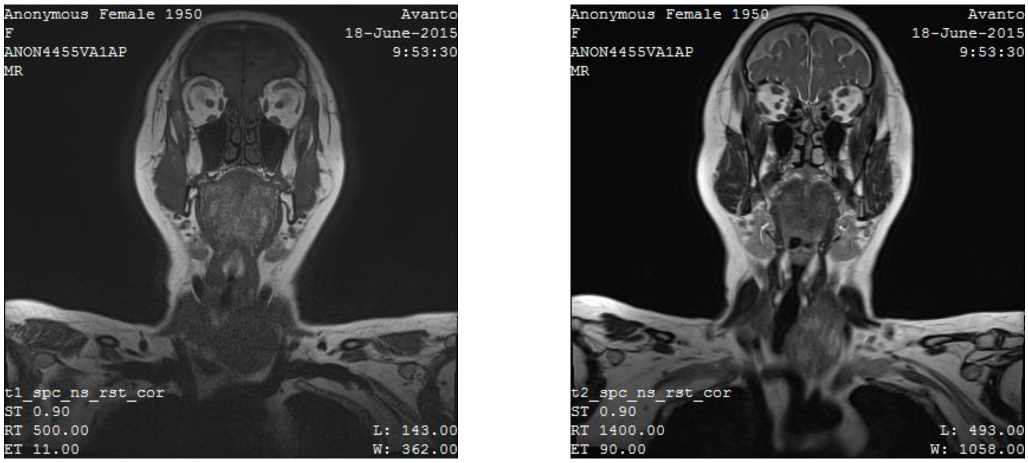

(a) T1 (b) T2

Figure 6: (a) and (b) show the difference between T1 and T2 weighted MRI images, respectively.

Essentially, MRI gives a proton density map for each slice which all together make up a 3D model of the body of interest. All the different proton densities represent different body parts and are shown as grayscales on the MR image. The lightest colour refers to the lowest density, and pure air is on the other end of the scale and shows up as dark in the images.

The imaging process takes from 20-60 minutes, and the patient has to lay still for the entire time to achieve good quality images. Another disadvantage is that all metal has to be removed from the patient because of the strong magnetic field utilized in the procedure. Hence patients with metal in the body due to e.g. previous surgeries cannot undergo MRI. The main advantages of MRI are that it is a completely harmless procedure, the different soft tissues show up detailed, and the images can be taken in coronal, axial and sagittal slices [25].

1.4.2 CT

A CT scanner emits X-rays into the body, and creates a picture based on how the photons in the X-rays are absorbed or redirected from the structures they pass through in the body. The degree to which an X-ray beam is reduced by the structure is called attenuation, and the grayscale image represents this in Hounsfield units (HU). HU is defined by

$$HU = 1000 \cdot \frac{\mu_P - \mu_W}{\mu_W} \tag{1}$$

where μ_P and μ_W are the mean X-ray attenuation coefficients of the tissue in the pixel and water, respectively [8]. On the Hounsfield units scale, air defines the lower limit at -1024 HU, water is at 0 HU, and at the upper limit, tooth enamel, is at 3072 HU [8].

The main advantages of CT are the short scanning time (only a few minutes depending on the machine itself) and the representation of the bony structures. The disadvantages are that soft tissue does not show up in detail and that it is not a completely harmless procedure as it exposes the patient to ionizing radiation [8].

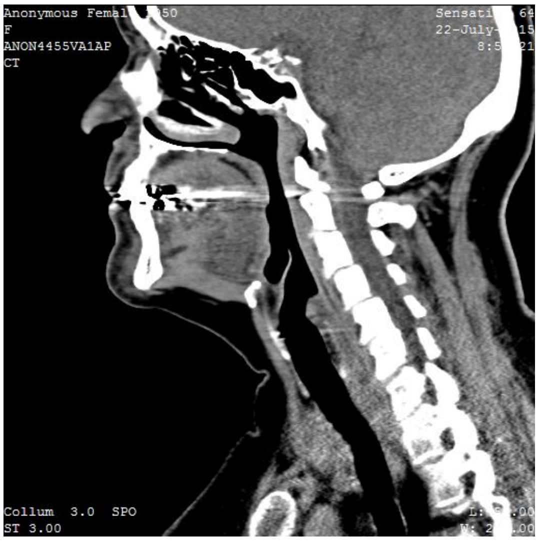

Figure 7: CT image of the upper airway, sagittal plane.

As seen in Fig. 7, the bony structures stands out as white, air stands out as black, and all the soft tissue appears as gray. Comparing the MRI (Fig. 6) and CT (Fig. 7) it is clear that the detail level of the soft tissue is much lower in CT than in the MR images.

1.5 Geometry Retrieval

Geometry retrieval from the medical images can be done by segmentation. As the image sets contain information about more than just the upper airway, the region of interest must be separated from the rest. During segmentation, each of the voxels in the images get labelled based on specified characteristics. All the voxels with the same label can then be extracted all together making up a model of an anatomical feature [8].

Segmentation can be done both automatically and manually and there exist several software making the process easier. The commercial software MIMICS [26] is widely used, but there are also several free softwares such as ITK-SNAP [27] and Slicer [28].

1.6 Grid Generation

The flow physics can be represented by a set of mathematical equations. Grid generation is in essence dividing the entire geometry into smaller grid cells to be able to solve flow equations over the domain. To simulate the flow field on a geometry, such as the upper airway, these mathematical equations are applied to every grid cell. In order to obtain good and accurate results, the grid is of great importance. The type of grid cells, size of the cells and the grid structure define where, and how many times the equations are solved [8].

1.6.1 Grid Characteristics

There are numerous possibilities for grid generation. The grid can either be structured or unstructured. A 3D structured grid is made up of hexahedrons while an unstructured grid is commonly made up of triangles and tetrahedra in irregular patterns. An unstructured grid is better in use for irregular geometries such as the upper airway. In addition to triangles and tetrahedra, the unstructured grid can consist of other cell types. Often a hybrid grid (several different cell types) is needed to fit the geometry in the best way [8].

1.6.2 Evaluation of grid quality

Generating a grid is quite easy with the softwares available, but generating a quality grid, however, is more challenging.

To ensure that the grid is of good quality, the cell shapes can be evaluated based on a series of measures. The aspect ratio defined the base to height ratio of a cell element. It can be within the range of 0 to 20, where 0 is a perfect element, and 20 refers to an extremely stretched element. Most preferable, the aspect ratio should be within the range of 0.2 and 5 in the interior region of the grid. Near the wall, however, the aspect ratio can be relaxed [8]. The same formation of the element is measured with the maximum corner angle. Skewness is a measure of how skewed the elements are. The ratio is from 0 to 1, and should be within the range of 0 to 0.25 to be considered good. Another indication of the twisting of the element is the warping factor, where 0 indicates no twisting. The Jacobian Ratio indicate placement of the midside node. It ranges from 0 to 1000 for triangles and 0 to 100 for quadrilaterals, where 0 is optimal for both elements. Element quality refers to the quality and volume of the element, and range from 0 to 1 where 1 is a perfect element. The same range applies to the orthogonal quality [29].

The above mentioned ratios can be measured before simulations, but the best way to estimate the grid quality is by seeing how it affects the simulations. A good approach is to start with a coarse grid at first, and then refine the grid until the size of the cells no longer affects the simulations, and grid independence is reached.

2. Method

The physical changes in the upper airway after nasal surgery are documented for all the patients in the research project as they undergo CT and MRI both before surgery and three months after surgery. From the medical images obtained, the geometry of the upper airway can be extracted through segmentation, and converted to a solid body which a computational grid can be generated from.

2.1 Geometry Retrieval

From the medical images, the body scanned can be viewed as a volume. It is however not possible to get only a selected body part on the images, but the entire upper body - including the upper airway - is visible. The only part of interest for this project is the upper airway, and that part must therefore be retrieved and separated from the body surrounding it. This is done through the procedure presented in the following subsections.

2.1.1 Data Acquisition

The CT and MRI images were provided by the radiologic department at St Olav University Hospital. The patient is a 64 years old woman and. The CT was done with a Siemens Sensation 64 in the transverse plane. The pre-operative scan provided in 409 slices with a slice thickness of 1.0 mm, and the post-operative CT scan provided a total of 342 slices with a slice thickness of 1.5 mm, All of the 2D CT images consisted of 512x512 pixels. The volume of each voxel was 0.258 mm^3 pre-operative and 0.212 mm^3 post-operative.

The MRI was done with a Siemens Avanto in the coronal plane with 160 slices, each consisting of 384x384 pixels. The slice thickness was 0.90 mm and the voxel volume was 0.706 mm^3. This applies to both pre- and post-operative datasets.

2.1.2 Choice of medical image procedure

As the project title refers to, the geometry retrieval was going to be based on both CT and MRI, but the final model was made entirely from CT data. Originally the plan was to combine CT and MRI as it was expected that each of the imaging techniques had different information that were both needed to portrait the upper airway correctly. However, each of the different images sets contain enough information about the upper airway on their own. As explained in section 1.4.3, the main differences in the pictures obtained from CT and MRI are how detailed the soft tissues and the bony structures appear, but air shows up similar on both pictures. The data obtained from CT was chosen over the ones obtained from MRI because they were of better quality, more detailed and easier to segment. The voxel volumes from the CT and MRI scan were 0.212 mm^3 and 0.706 mm^3, respectively. As the MRI images have larger voxels, a larger area will have the same grayscale value, and the pictures become less detailed. Another factor that makes the CT images more accurate is the time it takes to obtain each CT and MRI series. Obtaining the MR data takes about 20 minutes so the patient tend to move and/or fall asleep during this time causing movement artefacts on the images. CT on the other hand only take about a minute to obtain, hence the patient is not moving as much during this short time, which improves the quality of the image.

Another advantage of choosing CT is evident when the goal is to make an algorithm to produce several models for comparative air flow modelling. On the CT-images, the different internal structures are represented in terms of HU-values. As the HU-scale is a standardized scale, these values are the same for different patients. When a HU-range for air is defined, it can be applied on all image series - even for different patients. The grayscale representing the structures on an MRI image is not standardized. The values on the different image series from MRI are not comparable, and a new decision on what the range should be have to be taken for each case [30].

The choice of not including MRI in the geometry retrieval is also supported by the fact that previous work that included reconstruction of the upper airways have been done based on CT with great success [31–35].

2.1.3 Segmentation

To perform the segmentation the freeware ITK-SNAP 3.2.0 [27] was used to make a 3D model of the upper airway after surgery. There exist several softwares, but ITK-SNAP has been chosen for this project work as it is free and has been given good credits [27,36]. ITK-SNAP is userfriendly and includes only the main functions needed for segmentation of anatomical structures.

The DICOM (Digital Imaging and Communications in Medicine) files obtained from CT-scans after surgery were imported to ITK-SNAP as DICOM image series (Fig. 8). The post-operative image set was chosen as the patient had an open mouth in the pre-operative scan, but a closed mouth in the post-operative scan. This will be discussed further on in the report.

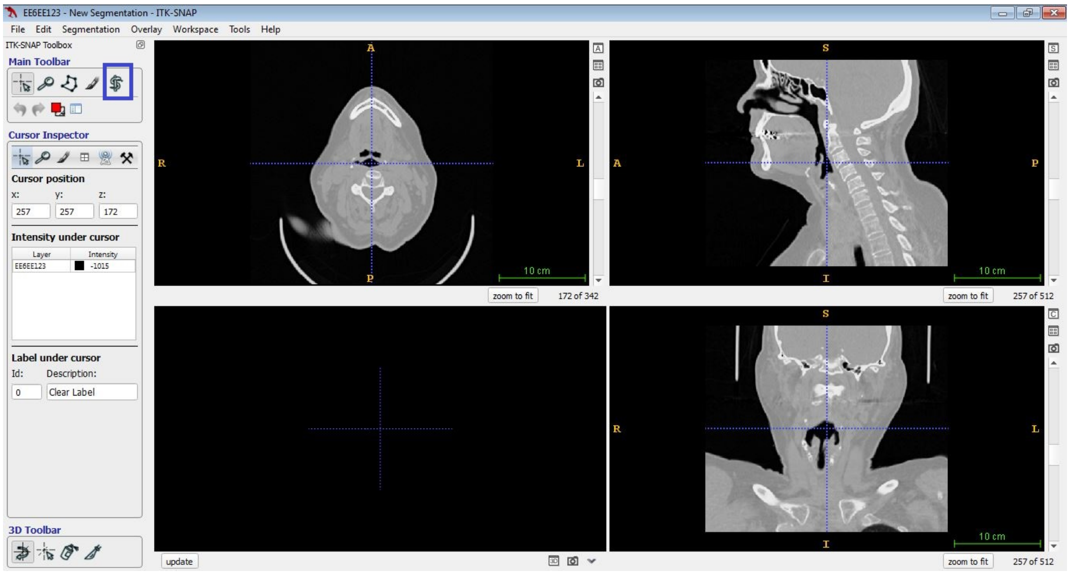

Figure 8: The loaded DICOM files as they appear in ITK-SNAP.

The loaded files are viewed clockwise as three 2D image series in the transverse, sagittal and coronal planes (Fig. 8), respectively. The segmented volume will appear in the lower left corner, but as nothing is segmented at this point, only the axes are visible. Under each image series, it is shown which slice and where in the pixel-matrix you are. The anatomical planes are also marked on all four sides of the images (see also Fig. 2).

To perform the automatic segmentation, the Active Contour Segmentation (Snake) mode was chosen in the Main Toolbar (marked with a blue square in the left corner in Fig. 8), and a region of interest to segment within was defined. This is done by adjusting the red square that appears in all of the three image-windows once "snake mode" is chosen. These 3D boxes can be adjusted in all anatomical planes. In Fig. 9, the pharynx have been chosen as the region of interest, and is marked with a red dashed line.

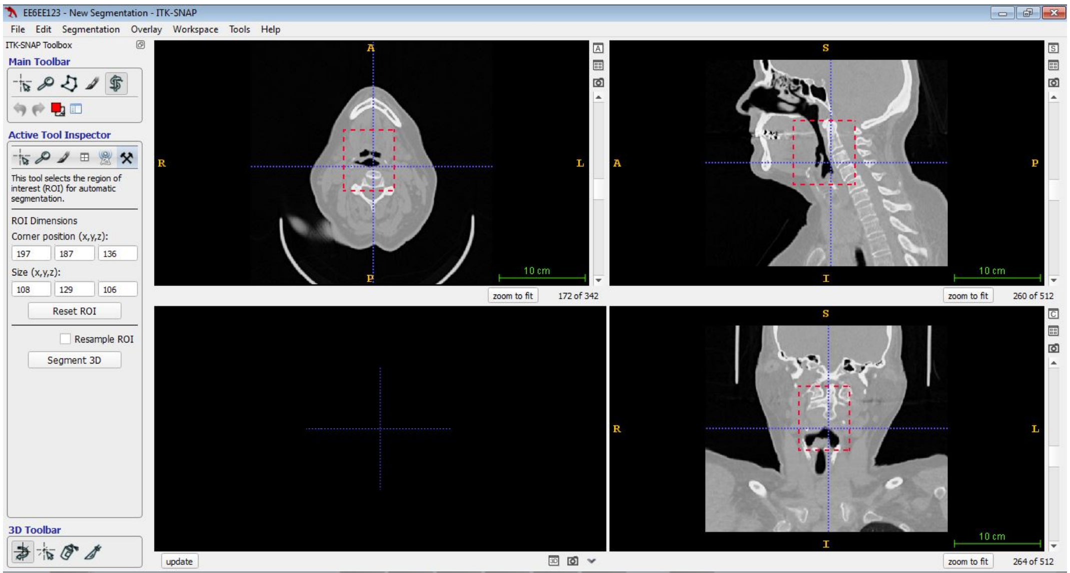

Figure 9: The loaded DICOM files in ITK-SNAP with a chosen region of interest marked with a red dashed line.

After the region of interest is defined, the ”segment 3D” button is pushed, and a new window with only the region of interest shows up as seen in Fig. 10. As before, the slice you are at can be seen under the image, but now only the images within the defined region are available.

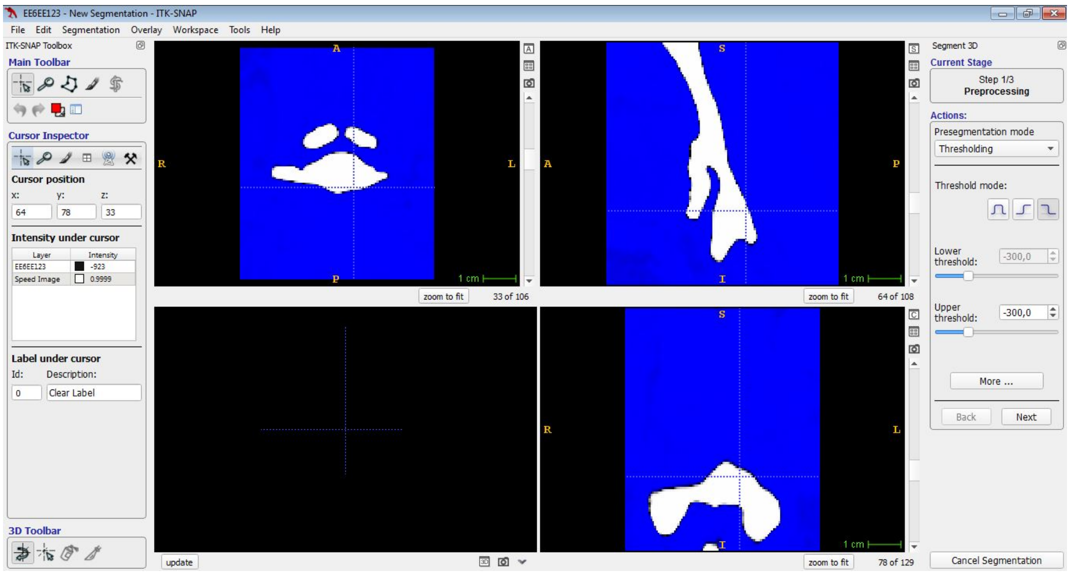

Figure 10: The presegmentation step 1/3 in ITK-SNAP showing the region of interested with the applied thresholding values.

As seen in Fig. 10, a new toolbar appears on the right side of the screen. One of the following presegmentation modes must be selected; thresholding, edge attraction, clustering or classification. For this project, thresholding was chosen.

This is because air defines the lower limit on the HU-range, and only the upper threshold value needs to be defined. Air also stands out from the gray tissues around. When using thresholding, an upper, lower or range of HU-value can be chosen. In Fig. 10 -300 is chosen as the upper limit, and everything that is above that limit is blue. The white parts covers the area that holds HU-values from -300 and below. The choice of setting the upper limit to -300 is explained below.

After clicking next, the next step of the segmentation is to place one or more seeds at the geometry for it to grow into the parts that are going to be segmented. The seed is shown as a red circle in Fig. 11. The seed must be placed at least partly on the white area, but it grows both inward and outward so it will adjust if it is partly placed outside the part of interest. Note that also the original CT-slice are shown in Fig. 11 as it has been chosen by the user by selecting ”more” in Fig. 9.

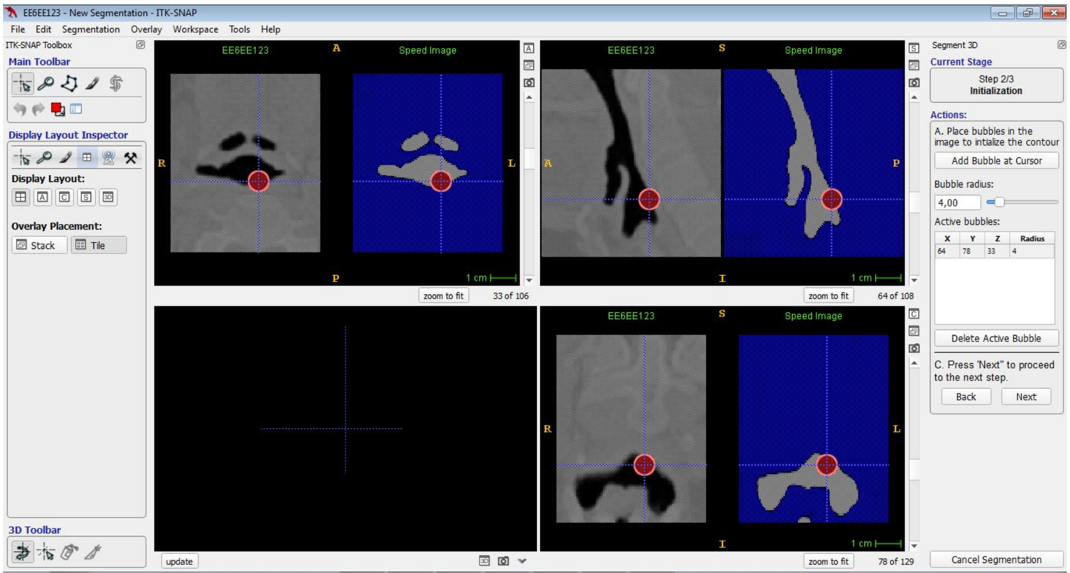

Figure 11: The ITK-SNAP window step 2/3 - with a (red) seed placed.

The next step of the segmentation is letting the seed grow into all the voxels within the defined thresholding range as a snake, see Fig. 12. This will go on for as many timesteps and iterations as chosen by the user. In this project, about 800 iterations were used with a timestep of 5.

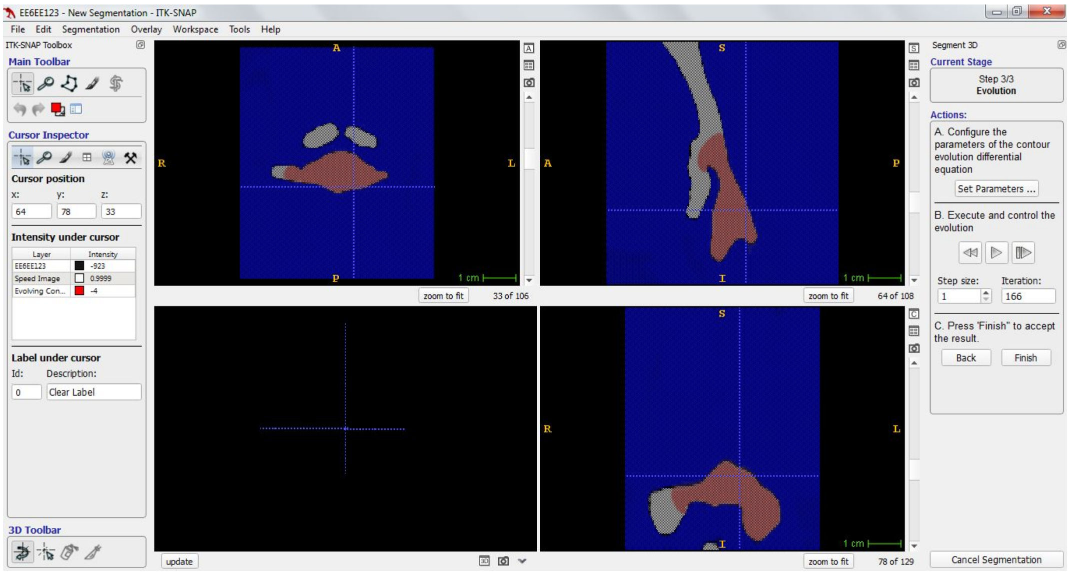

Figure 12: The ITK-SNAP window step 3/3 - showing the evolution of the "snake".

The result of the segmentation can be seen in Fig. 13, marked as red. In the lower left corner, a 3D representation of the segmented volume is shown. Note that only the slices that were in the region of interested have been segmented.

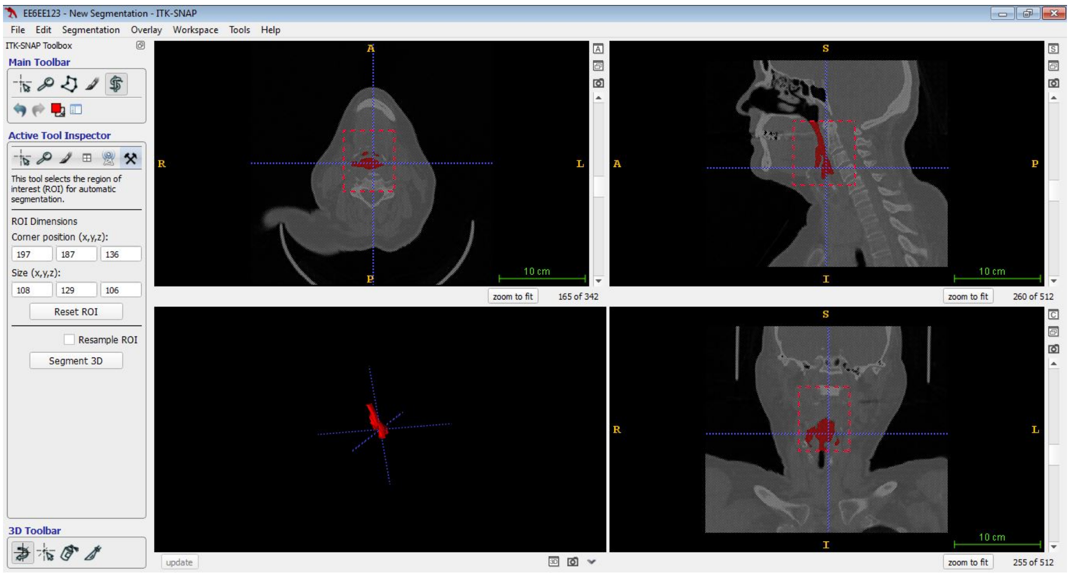

Figure 13: The ITK-SNAP window showing the result of the segmentation procedure. The red are represents the segmented volume.

The choice of -300 as the upper HU-limit is based upon a trial and error approach with initial values found in the literature. The lower limit of -1024 corresponding to air, defines the HU-scale, but there seem to be no clear agreement of what the upper limit should be.

Upper HU-values such as -300 [35] , -400 [31],-460 to -470 [37] and -587 [36] have been used in previous work, and were tested in this study. It turned out that using the lowest upper HU-value suggested for air resulted in a model with an inconsistent nasal cavity. Another issue with having too low upper limit is that even if the nasal cavity end up being consistent, the low upper limit results in a too small cross sectional area, such as only one pixel. A cross sectional area that is too small will make meshing and flow simulations difficult. The limit of -300 HU was tried to make a new model. This limit also gave a segmented volume which did not reflect the real anatomy. The nasal cavity had smaller parts that were not connected to the rest, and at the same time too much were included in the segmented volume. An example of this is that part of the septum showed up as air and connected the two nasal cavities where they in real life were not. A comparison of the effect of the upper HU-limit can be seen in Fig. 14, where the red color shows the segmented volume.

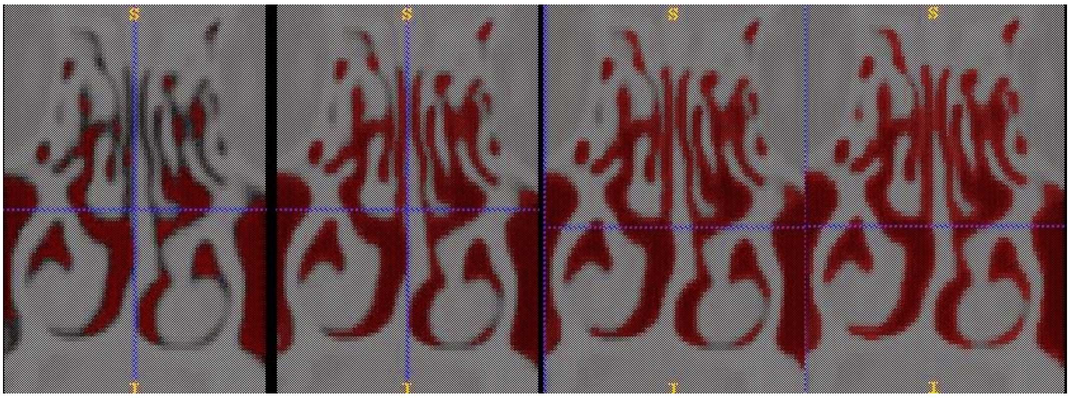

Figure 14: Comparison of segmentation of a coronal slice in the nasal cavity, from left to right segmented with an upper HU-value of -800, -500, -400 and -300, respectively

The trial approach was to automatically segment with -300 HU as the upper limit as this seemed to be giving the best result, and then manually segment the rest. When manually segmenting, the approach was to go through all the slices in the transverse plane and make sure the airway was segmented correctly in each of these slices, and make the necessary changes. After this the same was done with the slices in both the sagittal and lateral planes. Manual segmentation is time consuming, but necessary to get a realistic model.

After the segmentation was performed, the result was discussed with both a radiologist (K.A. Kvistad) and a surgeon (M. Moxness). The outcome of this discussion was to exclude all the paranasal sinuses (maxillary sinuses are marked as 1 and 2 in Fig. 15), and to limit the geometry with the outer borders marked with blue lines in Fig. 15a. Another ting that was hard to catch without having medical insight was what looked like part of the flow area around the turbinate was in fact an unusual nasolacrimal duct (tear duct) (marked as 3 in Fig. 15b) that should be excluded.

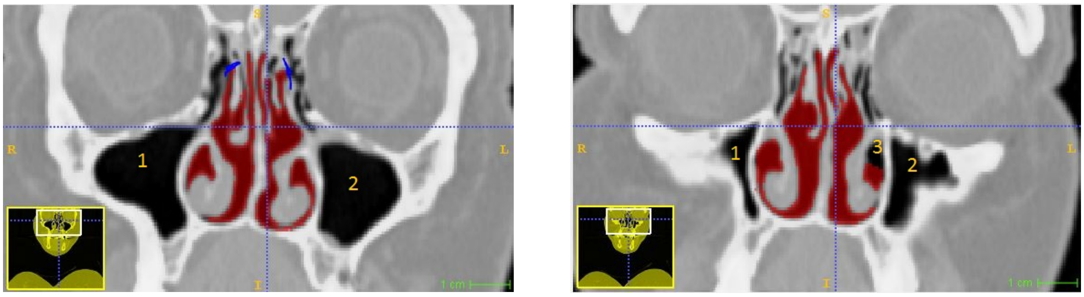

(a) (b)

Figure 15: Coronal CT scan of the nasal cavity with maxillary sinuses and nasolacrial duct marked as 1,2 and 3. The blue lines indicates the outline of the segmentation.

2.1.4 Conversion from surface mesh to solid body

The segmented volume from ITK-SNAP [27] is presented as a surface mesh and saved as a stereolithography (STL) file, which gives only the surface geometry represented by small triangulated faces. To be able to generate a grid for flow modelling, the geometry model must be a solid body - not just a surface mesh. To convert the STL file to a solid body, the freeware Free-CAD 0.15 [38] was used. In Free-CAD the STL file was imported and then converted to a STEP file (Standard for The Exchange of Product model data) with a built in function in the program [39]. This solid body could then be imported to ANSYS DesignModeler 16.2 and meshing for further work.

2.2 Grid Generation

The grid generation was done in ANSYS Meshing 16.2. The program was chosen as the grid generated in ANSYS Meshing easily can be imported to ANSYS Fluent as the project description refers to [40].

2.2.1 Choice of grid type

The geometry of the upper airway is complex and requires a great amount of grid cells. Previous simulations of the upper airway have been done with unstructured tetrahedral grids [6, 31, 41–43]. These studies have used about 1 million grid cells. Not all of these studies included the nose and nasal cavities in the model implying that the number of grid cells for the geometry in this project should be at least 1 million.

2.2.2 Generating the grid

The first step was to divide the model into five parts to be able to grid the different parts separately. The partitioning was done in ANSYS DesignModeler and the result can be seen in Fig. 16. This model was then opened in ANSYS Meshing for grid generation.

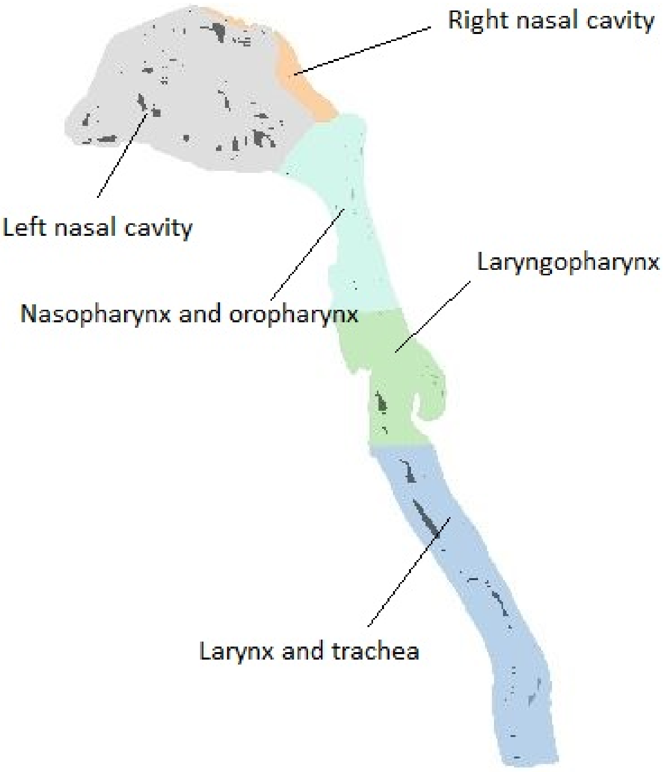

Figure 16: The parted model

The model was meshed in parts with no set element type. An unstructured grid was chosen because of the complex geometry. The solver preference was set to Fluent to make the grid importable to ANSYS Fluent for future flow simulations. The advanced sizing function using proximity and curvature was used to get a more detailed grid at all the edges of the geometry. The "automatic inflation" was used with a maximum of five inflation layers at the walls to get a finer grid near the walls.

3. Results

3.1 Geometry

The segmented volume from the patient after surgery can be seen in Fig. 17 and Fig. 18 where it is represented as a surface mesh made up of 241,296 triangles. The total segmented volume was $6.444{\cdot}10^4 mm^3$ and consisted of 303,467 voxels. The trachea has an unusual bend towards the right which is caused by a tumour next to the trachea.

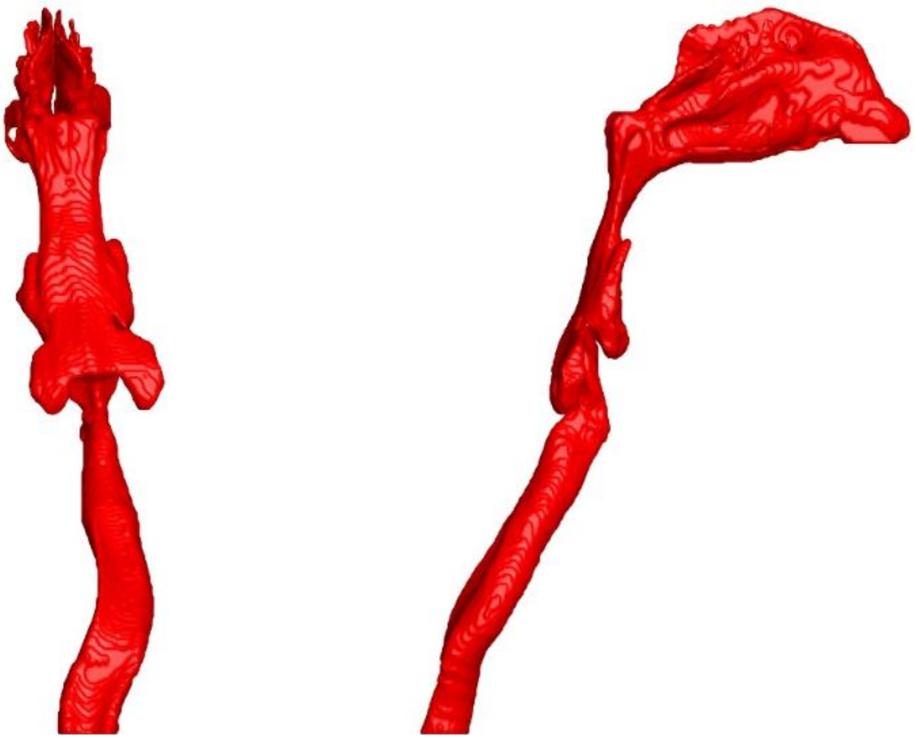

Figure 17: 3D view of the model seen from behind (left) and from the right side (right)

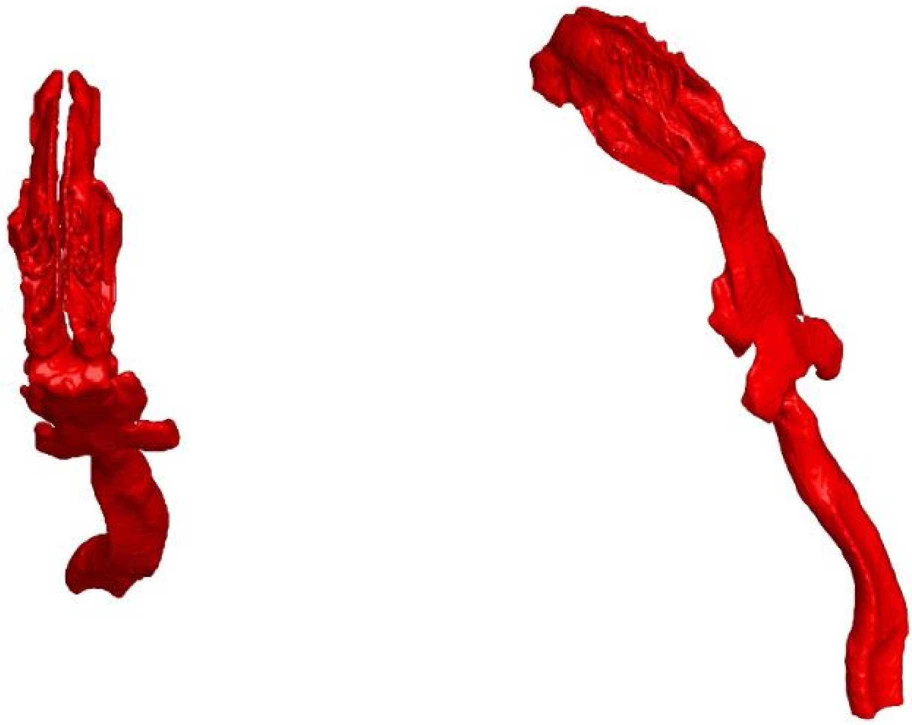

Figure 18: 3D view of the model seen from above (left) and from the left side (right)

A more detailed view of the nasal cavities can be seen in Figure 19 which shows coronal slices of the nasal cavity from the front and further posterior.

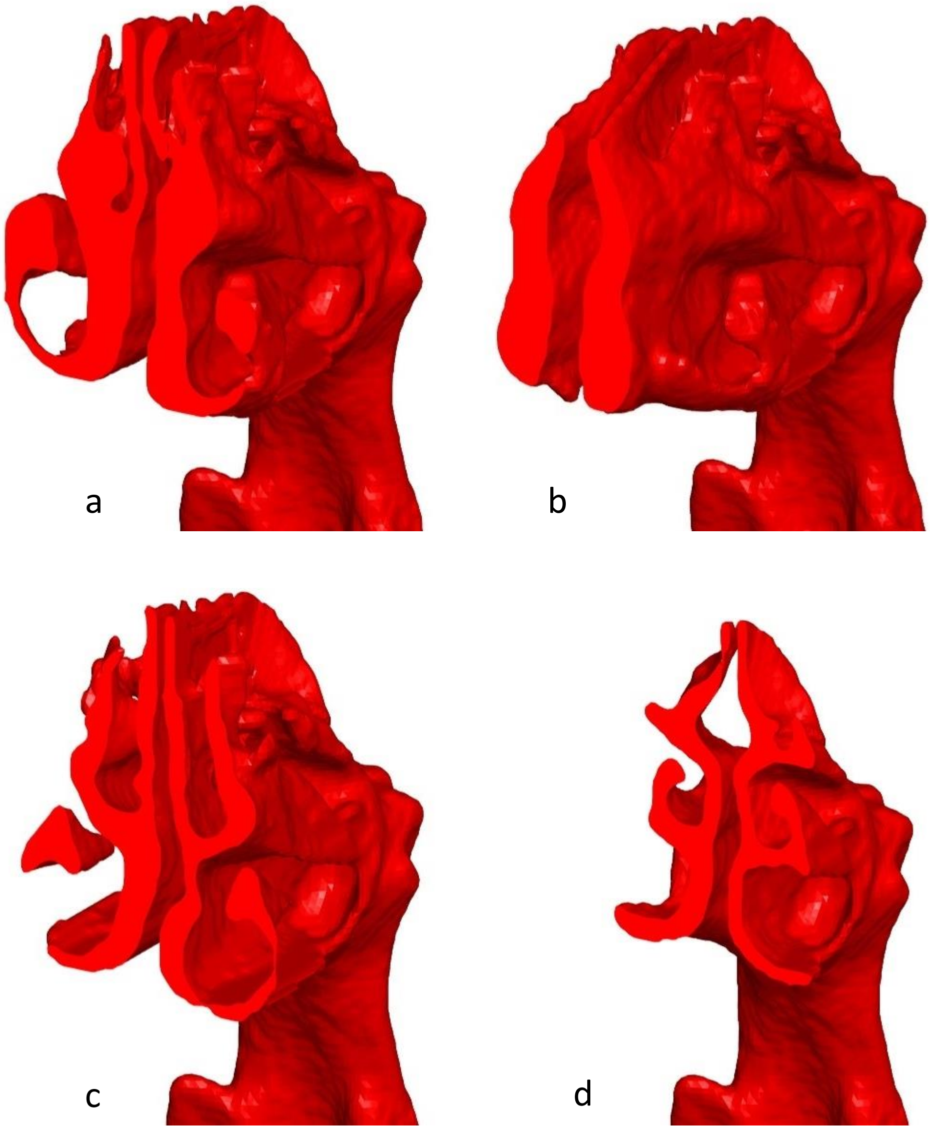

Figure 19: Coronal slices of the segmented volume in the nose and nasal cavities, viewed from the left side.

3.2 Grid

The final unstructured, hybrid grid consisted of 2,383,787 nodes and 5,955,285 elements. The mesh metrics are overall good (see section 1.6.2), and can be seen in Table 1.

Table 1: The average mesh metrics.

Mesh Metric	**Average Value**
Element Quality	0.4636
Aspect Ratio	5.3669
Jacobian Ratio	1.1104
Warping Factor	5.7899e-02
Maximum Corner Angle	89.73
Skewness	0.3725
Orthogonal Quality	0.80958

Details of the grid in the nasal cavity can be seen in Fig. 20. The grid is more detailed on the walls as a result of the automatic inflation adding inflation layers.

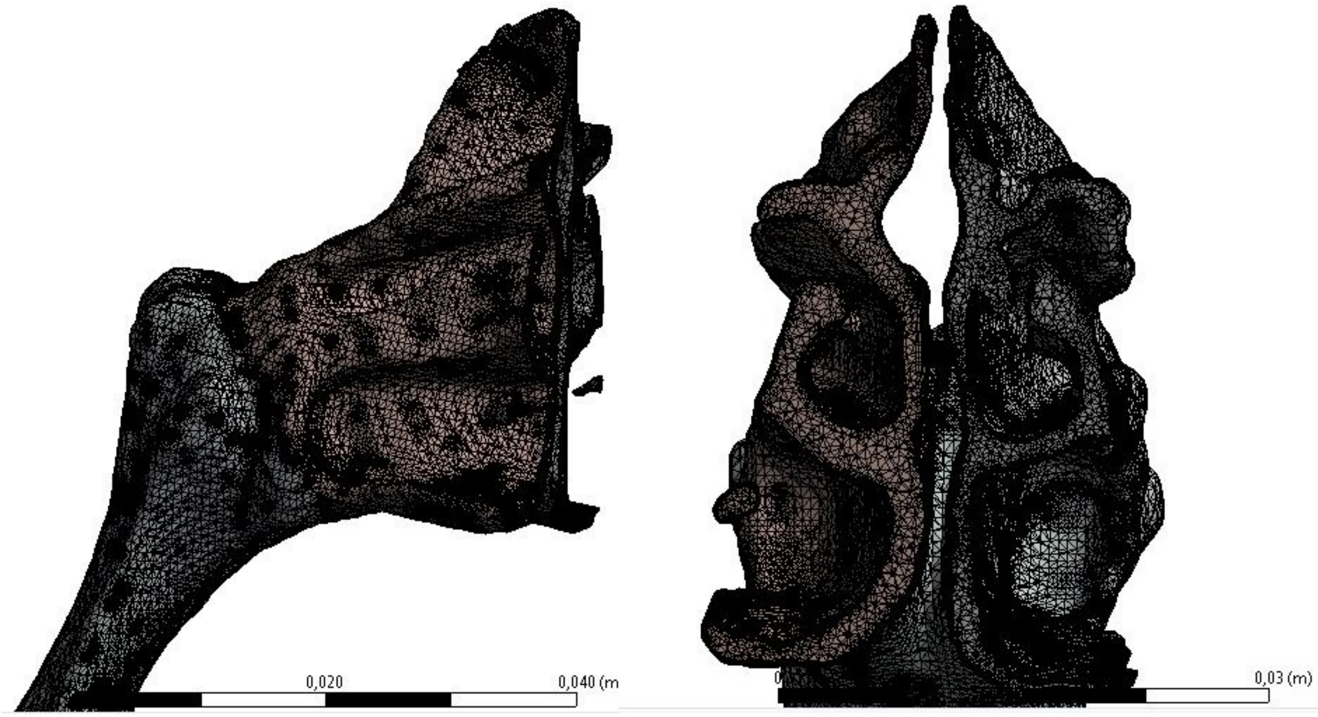

Figure 20: Details of the grid in the nasal cavities viewed from the right side (left) with the cross sectional area seen from the front and posterior (right).

Another view of the grid in the nasal cavities can be seen in Fig. 21. This cross sectional view shows the connection between the left and right nasal cavities and the nasopharynx. The elements in the nasopharynx are in general larger than those in the nasal cavities. It is a clear dividing between the different parts of the geometry, and the connections between the different grids are not so smooth as several elements from the nasal cavities connect into only one element in the nasopharynx. The same bad connection between the different parts can be seen in Fig. 22.

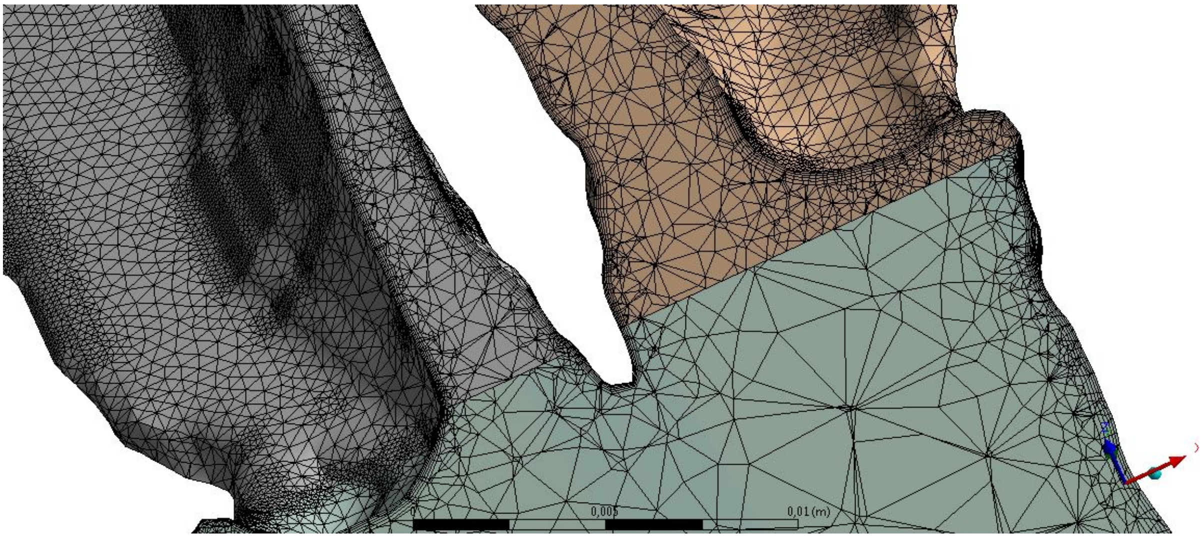

Figure 21: Details of the grid in the nasal cavities and nasopharynx. Cross sectional view seen from above.

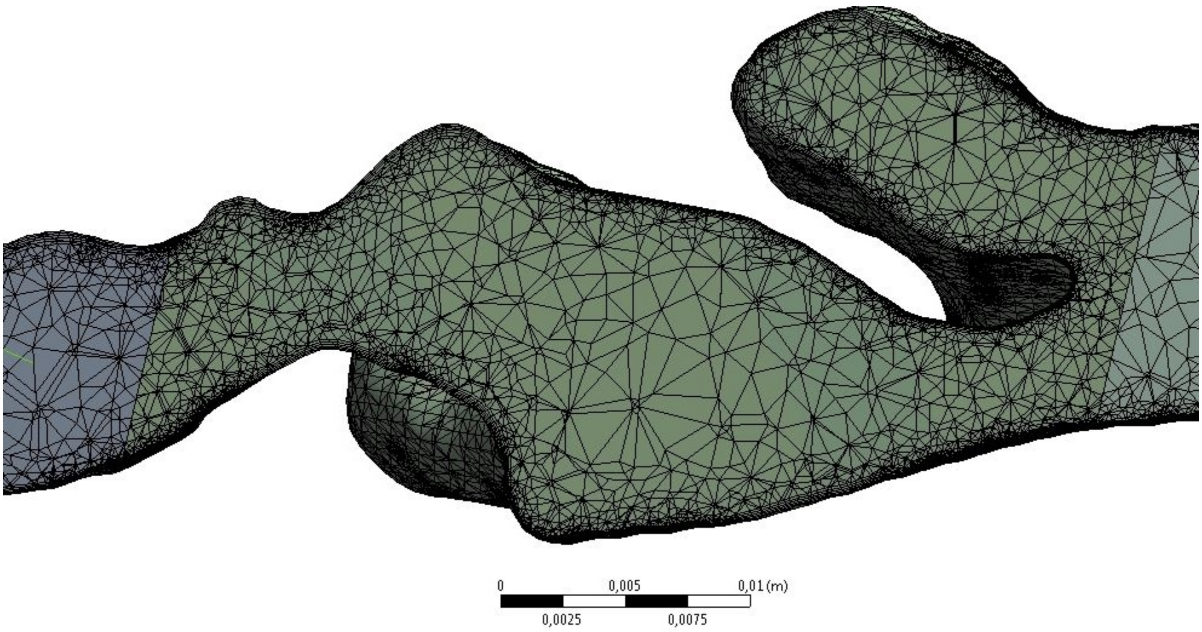

Figure 22: Details of the grid and connections between the oropharynx, laryngopharynx and larynx. Cross sectional view in the coronal plane.

3.3 Protocol

The following protocol (Fig. 23) is suggested for geometry retrieval from CT scans

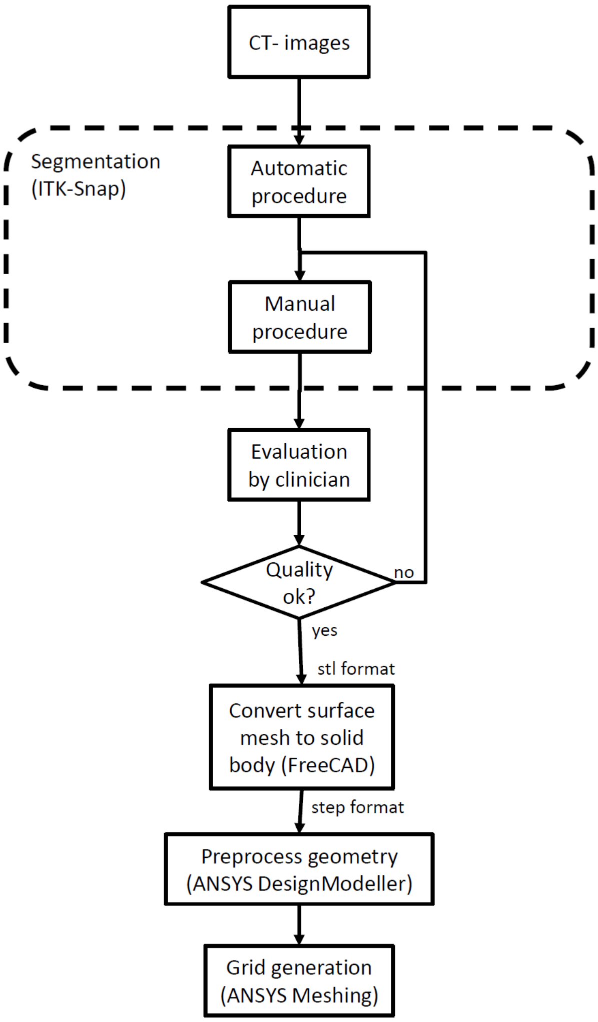

Figure 23: The suggested protocol for geometry retrieval from CT scans represented as a flow chart.

1. CT-imaging
   The first step is to obtain the CT-images, and this is done at the radiologic department at St Olav University Hospital. Each patient will undergo a total of four sets of CT. The protocol is the same both before and after surgery. To ensure that the images are comparable, the patient must be laying in the same position at all times, and a headrest will be used at all scans. The patient will undergo two scans both before and after surgery; one with closed mouth and one with open mouth. For the scans with an open mouth, the patients will be given a mouthpiece ensuring that the mouth is positioned the same. The images are saved as DICOM files.

2. Segmentation
   The segmentation will be done utilizing the software ITK-SNAP 3.2.0 [27]. The data set obtained from the CT scan where the patient has a closed mouth is loaded into ITK-SNAP 3.2.0 as a DICOM image series. The procedure consists of both automatic and manual segmentation. A more detailed description can be found in section 2.1.3.

   (a) Automatic Procedure
       The automatic segmentation is done with the Active Contour Segmentation ("Snake mode") tool and thresholding as presegmentation mode. The procedure goes as follows:

       i. Select region of interest.
       ii. Choose Active Contour Segmentation.
       iii. Choose thresholding with no lower limit and the upper limit as -300 HU.
       iv. Place seeds
       v. Choose timestep and stop the procedure after as many iterations as needed.

       This procedure is repeated until it does not give accurate results. Automatic segmentation gives overall good results for the larynx, pharynx and posterior nasal cavities. Examples of inaccurate results is prevalent in the nasal cavities. This can be that parts of the airway are not included as the segmented volume, or that parts of the nasal septum cartilage are included as the segmented volume. At this point one should continue on with the manual procedure.

   (b) Manual Procedure
       The manual procedure is to go through all the slices in the sagittal, axial and coronal planes. At each slice, the segmented volume is evaluated and necessary corrections are made by either add or remove to the segmented volume.

3. Evaluation by clinician
   A clinician such as a ENT (Ear-Nose-Throat) specialist, surgeon and/or radiologist should evaluate the segmented volume and compare with the data from the CT scans. Anatomy vary for each individual, and a clinician will be able to identify and locate different anatomical structures that should be included or excluded. Specifically of interest are the anatomy of the nasal cavities and all the small canals leading out to the paranasal sinuses.

4. Check Quality
   After segmentation and conversation with a clinician, a decision of whether or not the segmented volume is a good representation of the upper airways must be made. If changes should be made to the model, the segmentation procedure is repeated again. Most likely it will be small differences, and

those should be segmented manually.

5. Convert surface mesh to solid body
   The segmented volume from ITK-SNAP can be exported as a surface mesh (STL-file), but for grid generation a solid body (STEP-file) is needed. The conversion from surface mesh to solid body can be done with the software FreeCAD.

6. Preprocess geometry
   Preprocessing of the geometry can be done in ANSYS DesignModeler. The complexity of the geometry varies greatly throughout the upper airway, and the model should be partitioned into several parts with similar complexity. Suggestion of partitioning are as follows:
   (a) Left Nasal Cavity
   (b) Right Nasal Cavity
   (c) Nasopharynx and oropharynx
   (d) Laryngopharynx
   (e) Larynx and trachea

7. Grid Generation
   The partitioned model made in ANSYS DesignModeler is imported into ANSYS Meshing for grid generation. Several of the default values can be used, but suggested changes are as follows:
   (a) Physics Preference - CFD
   (b) Solver Preference - Fluent
   (c) Use Advanced Size Function - On: Proximity and Curvature
   (d) Use Automatic Inflation - Program Controlled

   After the grid generation, the mesh metrics should be checked in ANSYS Meshing to ensure they are within reasonable range as this indicate the quality of the grid. If they are not, changes should be made to mesh settings and/or preprocessing of the model.

4. Discussion

To be able to analyse the airflow in the upper airway before and after surgery, it is essential that the data before and after are comparable. For the patient in this project, the photos before and after surgery were not comparable. The images before surgery show a patient with an open mouth where the flow inlets are not only the nostrils, but also the mouth (Fig. 24a). After surgery, however, the patient has a closed mouth on the images. Hence the nostrils are the only flow inlets (Fig. 24b). In addition to introducing an extra flow inlet, an open mouth also causes the tongue to move further back and the oropharynx to narrow. This causes a geometrical difference that should not be there and will greatly impact the flow simulations. With a different amount of flow inlets and false geometry changes, it is difficult to see the impact intranasal surgery has on the airflow which is the aim of this project work. The need for a protocol for CT scanning was also pointed out by Ito et al. [35] who had difficulties comparing CFD results pre- and post-operative as the head position varied a lot in the pictures even though the mouth was closed.

(a) (b)

Figure 24: CT sagittal scans before and after surgery with open and closed mouth, respectively.

This problem could easily be solved by introducing a protocol to the image acquisition, and the project group has agreed on doing so. The issue with open and closed mouth does not only apply to the one patient included in this project work, but to several of the patients that have already undergone surgery, meaning that there may not be sufficient material to include them in the study. Ideally the CT should be taken with closed mouth to get the most realistic simulations. In optimal sleep with no obstructions, a person will naturally sleep with closed mouth - breathing only through the nose. To simulate the flow most realistically, and see weather or not the surgery improved AHI, the findings of the flow patterns with only the nares as flow inlets will show if it is actually feasible for the patient to sleep un-obstructed.

As a result of these findings, the patient will from now on undergo CT with both open and closed mouth before and after surgery. It will be ensured that the position of the head is the same in all image series by having a headrest. For the images with open mouth, the patient will have a mouthpiece ensuring the opening of the mouth to be similar in the scan before and after surgery. Taking twice as many CT image series exposes the patient to twice as much radiation, but the images with open mouth show the soft palate more clearly and are needed for other parts of the project.

A protocol for the geometry retrieval has also been obtained from this project work. Segmentation of the nasal cavity stood out as one of the most difficult parts and a source of error. The nasal cavity is very complex and there are no set rules to what should be part of the model or not as simplifications are made by excluding the paranasal sinuses. There are numerous smaller channels that vary from individual to individual and as some of the channels should be included, but not all, a specialist within medicine must be included in the segmentation process as pointed out in section 2.1.3 (see Fig. 15). Leaving out complex structures will reduce the computational time significantly, but these simplifications must not be done at the expense of giving inaccurate results. Leaving out the paranasal sinuses does most likely not affect the results and it is a common simplification in most papers describing simulation of the flow in the upper airways. However, the verification of the model could be done by comparing with and without the paranasal sinuses.

Validation of the model is at this point not possible as this is can only be done by simulating the flow. That was not a part of the project. The segmented airway volume can, however, be compared to other models from previous studies to make sure it is within reasonable range, but there will always be differences as there is no standard for the human body. This can therefore only catch large errors, and as the cross sectional area in the nasal cavities can be quite narrow at times, a small difference in volume makes a great change in the flow pattern. A better verification method is to compare the airway model for the same patient before and after surgery. As surgery is performed only in the nasal cavities, the volume of the pharynx and larynx should still be the same. In this case, the volumes before and after surgery were not comparable as mentioned because of the open mouth causing anatomical differences. The anatomy in the nasal cavity should not be as affected by the positioning in the CT scan as the pharynx or the larynx would, but as there has been done surgery there, it is no use to compare that specific volume. Another thing worth noting is that the nasal cycle (described in section 1.2.2) has not been taking into consideration. During each nasal cycle, one of the nasal passages is dominant causing the airflow to be asymmetrical. One of the nasal cavities will therefore appear larger than the other in the CT scan as they provide an instantaneous representation of the physiology. As a result of this, the difference between the left and right nasal cavities could be affected by the nasal cycle and should be taken into consideration.

Just like for the geometry, it is hard to say whether or not the grid is sufficient to give good results. It is fair to say the grid most likely will need further work, even though the mesh metrics were within reasonable range. The complexity of the geometry of the upper airway varies quite a lot throughout the model. In the nasal cavities, there are a lot of details requiring a fine mesh with small cells but, in for instance, the trachea the geometry is more pipe-like with wide cross sectional areas that do not require the similar fine grids. To decrease computational time the grid should vary throughout the model, but the connections must be better. At this point, information from several elements in the nasal cavities travel into only one big cell in the nasopharynx. Further, the information from one cell in the oropharynx travels at some places into several cells in the laryngopharynx. This also holds for the connection between the laryngopharynx and larynx. This will most likely affect the flow simulations and give unrealistic results.

For similar studies, the model (including geometry, grid and flow simulations) has been verified by comparing the simulation with either experimental data from a prototype made of the computational model [4, 6, 41] or by comparing the flow results with real data [42]. The trend seems to be that flow simulations are needed for validation. Hence further work is needed to be able to validate the model in this report. However, the mentioned studies have all showed good correlations between the simulated and experimental results and indicate that there is great potential for using CFD to predict the outcome of upper airway surgery.

5. Conclusions

From this project work, protocols for image acquisition, geometry retrieval and grid generation have been established.

Both CT and MRI data of the patient were available for geometry retrieval, but the pre- and post-operative images were not comparable for airflow simulations. Some image sets were taken of a patient with an open mouth, and some with a closed mouth. When the mouth is open, it becomes a flow inlet, in addition to the two nostrils, and makes the tongue fall back toward the oropharynx. This causes a geometrical difference and narrowing of the pharyngeal airway that would not appear if the mouth was closed. These findings have led to a protocol for the image acquisition. According to the new protocol, each patient will undergo a total of four CT scans; with an open and closed mouth both before and after surgery.

A protocol for retrieving the geometry from medical images has been established. Even though both CT and MR data pre and post surgery were available for the patient, the model is entirely based on CT data. As each dataset from CT and MRI contains enough information about the upper airway on its own, there was no need in using both for the geometry retrieval. CT was chosen over MRI because the images contain more data (smaller voxels) and have less movement artefacts. The segmentation was done in ITK-SNAP 3.2.0. Segmentation of the larynx and the pharynx could be done almost entirely automatically, but the nasal cavity and the nose required manual work because of the complex anatomical structures. In addition to this, it is also necessary that a clinician evaluates the segmentation, as there are anatomical differences between every patient.

Validation of the model is challenging at this point. Previous studies validate their models (both geometry and grid) by comparing the flow simulations with experimental results. At this point there is still work left before a flow simulation can be made and possibly compared with experimental data. This means that the modelling is in fact at a point where it is not yet possible to estimate the accuracy of the model and more work is needed.

6. Further Work

As there exist several other segmentation tools it would be interesting to try those and compare with ITK-SNAP. Two suggestions for such tools are MIMICS as it is widely used for segmentation of the upper airway and Slicer which is used at St Olav University Hospital. It would be interesting to compare the user-friendliness and time spent on segmentation in addition to the results obtained by using the same algorithm.

More work on grid generation could also be of interest to possibly decrease the number of grid cells. Suggestions are to partition the model differently for individual meshing to see how this affects the grid. Attention should also be paid to the connections between the grid of the different parts. To validate the model made, and possibly reach mesh independence, the airflow through the geometry of the upper airway can be simulated in ANSYS Fluent.

Further work for this project work in WP4 is to generate models of more patients once the CT are being done according to the new scanning protocol. The airflow through the different models can be simulated and the results from the simulations are expected to indicate whether or not the patient's AHI should improve after surgery. Results from the simulations can then be compared with the actual outcome of the surgery and indicate the accuracy of the computer model.

Another way to validate the geometrical model, grid and eventually the simulation of the flow is to make an in-vitro model from the computer model and do experiments as seen in similar reconstructions of the upper airway.

References

[1] "Prosjektbanken - modellering av obstruktiv søvnapne ved fluid-strukturinteraksjon i de øvre luftveiene." https://www.forskningsradet.no/prosjektbanken/!/project/231741/en.

[2] "Modeling of Obstructive Sleep Apnea by Fluid-Structure Interaction in the Upper Airways." http://osas.no/description.

[3] M. H. Moxness and S. Nordgard, "An observational cohort study of the effects of septoplasty with or without inferior turbinate reduction in patients with obstructive sleep apnea," *BMC Ear, Nose and Throat Disorders*, vol. 14, no. 1, p. 11, 2014.

[4] G. Mylavarapu, S. Murugappan, M. Mihaescu, M. Kalra, S. Khosla, and E. Gutmark, "Validation of computational fluid dynamics methodology used for human upper airway flow simulations," *Journal of Biomechanics*, vol. 42, no. 10, pp. 1553 – 1559, 2009.

[5] R. Löhner, J. Cebral, O. Soto, P. Yim, and J. E. Burgess, "Applications of patient-specific cfd in medicine and life sciences," *International Journal for Numerical Methods in Fluids*, vol. 43, no. 6-7, pp. 637–650, 2003.

[6] M. Zhao, T. Barber, P. Cistulli, K. Sutherland, and G. Rosengarten, "Computational fluid dynamics for the assessment of upper airway response to oral appliance treatment in obstructive sleep apnea," *Journal of Biomechanics*, vol. 46, no. 1, pp. 142 – 150, 2013.

[7] Blausen.com staff, " Blausen Gallery 2014 The Respiratory System." Wikiversity Journal of Medicine https://en.wikiversity.org/wiki/Wikiversity$Journalof_Medicine/Blausengallery$2014.

[8] J. Tu, K. Inthavong, and G. Ahmadi, *Computational Fluid and Particle Dynamics in the Human Respiratory System*. Springer, 2013.

[9] B. H. Sinus, "Anatomy of the nose." http://www.beverlyhillssinus.com/nasal-and-sinus-disorders/nasal-polyps/.

[10] S. Standring and N. Borley, *Gray's Anatomy: The Anatomical Basis of Clinical Practice*. ClinicalKey 2012, Churchill Livingstone/Elsevier, 2008.

[11] A. Sahin-Yilmaz and R. M. Naclerio, "Anatomy and physiology of the upper airway," *Proceedings of the American Thoracic Society*, vol. 8, pp. 31–39, Mar 2011.

[12] C. S. Burwell, E. D. Robin, R. D. Whaley, and A. G. Bickelmann, "Extreme obesity associated with alveolar hypoventilationâa pickwickian syndrome," *The American Journal of Medicine*, vol. 21, no. 5, pp. 811 – 818, 1956.

[13] R. Kessler, A. Chaouat, P. Schinkewitch, M. Faller, S. Casel, J. Krieger, and E. Weitzenblum, "The obesity-hypoventilation syndrome revisited*: A prospective study of 34 consecutive cases," *Chest*, vol. 120, no. 2, pp. 369–376, 2001.

[14] H. Gastaut, C. Tassinari, and B. Duron, "Polygraphic study of the episodic diurnal and nocturnal (hypnic and respiratory) manifestations of the pickwick syndrome," *Brain Research*, vol. 1, no. 2, pp. 167 – 186, 1966.

[15] G. J. Gibson, "Obstructive sleep apnoea syndrome: underestimated and undertreated," *British Medical Bulletin*, vol. 72, no. 1, pp. 49–64, 2004.

[16] M. S. Aldrich, *Sleep Medicine : Normal Sleep and Its Disorders.* Oxford University Press, USA, April 1999.

[17] C. Sullivan, M. Berthon-Jones, F. Issa, and L. Eves, "Reversal of obstructive sleep apnoea by continious positive airway pressure applied through the nares," *The Lancet*, vol. 317, no. 8225, pp. 862 – 865, 1981. Originally published as Volume 1, Issue 8225.

[18] American Academy of Sleep Medicine, "Sleep-related breathing disorders in adults: Recommendations for syndrome definition and measurement techniques in clinical research," *SLEEP*, vol. 22, no. 5, pp. 667–689, 1999.

[19] R. B. Fogel, A. Malhotra, and D. P. White, "Sleep Â· 2: Pathophysiology of obstructive sleep apnoea/hypopnoea syndrome," *Thorax*, vol. 59, no. 2, pp. 159–163, 2004.

[20] I. Ayappa and D. M. Rapoport, "The upper airway in sleep: physiology of the pharynx," *Sleep Medicine Reviews*, vol. 7, no. 1, pp. 9 – 33, 2003.

[21] Science-Based Medicine, "Dental management of obstructive sleep apnea." https://www.sciencebasedmedicine.org/dental-management-of-obstructive-sleep-apnea/.

[22] N. AlGhanim, V. R. Comondore, J. Fleetham, C. A. Marra, and N. T. Ayas, "The economic impact of obstructive sleep apnea," *Lung*, vol. 186, pp. 7–12, 2008.

[23] M. Camacho, V. Certal, S. E. Brietzke, J.-E. C. Holty, C. Guillemeniault, and R. Capasso, "Tracheostomy as treatment for adult obstructive sleep apnea: A systematic review and meta-analysis," *The Laryngoscope*, vol. 124, pp. 803–811, 2014.

[24] N. B. Powell, "Contemporary surgery for obstructive sleep apnea syndrome," *Clin Exp Otorhinolaryngol*, vol. 2, pp. 107–114, Sep 2009. 19784401[pmid].

[25] N. B. Smith and A. Webb, *Introduction to Medical Imaging : Physics, Engineering and Clinical Applications.* Cambridge University Press, 2010.

[26] Materialise, "Mimics." http://biomedical.materialise.com/mimics.

[27] P. A. Yushkevich, J. Piven, H. Cody Hazlett, R. Gimpel Smith, S. Ho, J. C. Gee, and G. Gerig, "User-guided 3D active contour segmentation of anatomical structures: Significantly improved efficiency and reliability," *Neuroimage*, vol. 31, no. 3, pp. 1116–1128, 2006.

[28] "3d slicer." https://www.slicer.org/.

[29] Sharcnet, "Index of/software/ansys/16.0/en-us/help/wb$_m$*sh."https* : *//www.sharcnet.ca/Software/Ansys*/16.0/*en* − *us*/*help*/*wb*$_m$*sh*/.

[30] A. Madabhushi and J. K. Udupa, "New methods of mr image intensity standardization via generalized scale," *Med. Phys.*, vol. 33, no. 9, pp. 3426–3434, 2006.

[31] J. D. Backer, O. Vanderveken, W. Vos, A. Devolder, S. Verhulst, J. Verbraecken, P. Parizel, M. Braem, P. V. de Heyning, and W. D. Backer, "Functional imaging using computational fluid dynamics to predict treatment success of mandibular advancement devices in sleep-disordered breathing," *Journal of Biomechanics*, vol. 40, no. 16, pp. 3708 – 3714, 2007.

[32] G. Mylavarapu, M. Mihaescu, L. Fuchs, G. Papatziamos, and E. Gutmark, "Planning human upper airway surgery using computational fluid dynamics," *Journal of Biomechanics*, vol. 46, no. 12, pp. 1979 – 1986, 2013.

[33] M. Lu, Y. Liu, J. Ye, and H. Luo, "Large eddy simulation of flow in realistic human upper airways with obstructive sleep," *Procedia Computer Science*, vol. 29, pp. 557 – 564, 2014. 2014 International Conference on Computational Science.

[34] N. B. Powell, M. Mihaescu, G. Mylavarapu, E. M. Weaver, C. Guilleminault, and E. Gutmark, "Patterns in pharyngeal airflow associated with sleep-disordered breathing," *Sleep Medicine*, vol. 12, no. 10, pp. 966 – 974, 2011.

[35] Y. Ito, G. C. Cheng, A. M. Shih, R. P. Koomullil, B. K. Soni, S. Sittitavornwong, and P. D. Waite, "Patient-specific geometry modeling and mesh generation for simulating obstructive sleep apnea syndrome cases by maxillomandibular advancement," *Mathematics and Computers in Simulation*, vol. 81, pp. 1876–1891, May 2011.

[36] A. Weissheimer, L. M. de Menezes, G. T. Sameshima, R. Enciso, J. Pham, and D. Grauer, "Imaging software accuracy for 3-dimensional analysis of the upper airway," *American Journal of Orthodontics and Dentofacial Orthopedics*, vol. 142, no. 6, pp. 801 – 813, 2012.

[37] H. Nakano, K. Mishima, Y. Ueda, A. Matsushita, H. Suga, Y. Miyawaki, T. Mano, Y. Mori, and Y. Ueyama, "A new method for determining the optimal ct threshold for extracting the upper airway," *Dentomaxillofacial Radiology*, vol. 42, no. 3, 2013.

[38] "Freecad (version 0.15)." http://www.freecadweb.org/.

[39] K. Froyn, "Tutorial: Edit a 3d stl from thingiverse with freecad." https://www.youtube.com/watch?v=avVNfIswkMU, 2013.

[40] "Patient specific modeling for prediction of success of osas surgery." http://osas.no/work-package/wp4.

[41] C. Xu, S. Sin, J. M. McDonough, J. K. Udupa, A. Guez, R. Arens, and D. M. Wootton, "Computational fluid dynamics modeling of the upper airway of children with obstructive sleep apnea syndrome in steady flow," *Journal of Biomechanics*, vol. 39, no. 11, pp. 2043 – 2054, 2006.

[42] S.-J. Sung, S.-J. Jeong, Y.-S. Yu, C.-J. Hwang, and E.-K. Pae, "Customized three-dimensional computational fluid dynamics simulation of the upper airway of obstructive sleep apnea," *The Angle Orthodontist*, vol. 76, no. 5, pp. 791–799, 2006.

[43] S.-J. Jeong, W.-S. Kim, and S.-J. Sung, "Numerical investigation on the flow characteristics and aerodynamic force of the upper airway of patient with obstructive sleep apnea using computational fluid dynamics," *Medical Engineering Physics*, vol. 29, no. 6, pp. 637 – 651, 2007.